Textile & Leather Review

ISSN 2623-6281 | www.tlr-journal.com | 10.31881/TLR

An Accurate Discharge Detection Method Based on PDDA and Silicon-Based UV Sensors

Yong Liu, Yangyang Liu, Chunlei Dong

How to cite: LIU Y, LIU Y, DONG C. An Accurate Discharge Detection Method Based on PDDA and Silicon-Based UV Sensors. Textile & Leather Review. 2026; 9:3303-3315. https://doi.org/10.31881/TLR.2026.3303

How to link: https://doi.org/10.31881/TLR.2026.3303

Published: 25 April 2026

An Accurate Discharge Detection Method Based on PDDA and Silicon-Based UV Sensors

Yong Liu*,Yangyang Liu, Chunlei Dong
State Grid Hebei Electric Power Co., Ltd., Shijiazhuang 052100, Hebei, China
*lvhuaqing013@163.com

Article
https://doi.org/10.31881/TLR.2026.3303
Published 25 April 2026

ABSTRACT

Silicon-based ultraviolet sensors enable direct and non-contact monitoring of true discharge by capturing ultraviolet emission patterns. This monitoring is of significant value for the electrical safety of industrial facilities, such as textile production lines, where discharge events can lead to equipment failure or safety hazards. However, discharge targets in silicon-based UV images are often weak and small, and they are easily confused with background noise. To address these challenges, this paper proposes PDDA, a discharge detection method built on YOLOv8. PDDA introduces an EMA attention module into the bottleneck to enhance pixel-level feature weighting, replaces the original neck with a Cross-level Context Fusion Module to strengthen multi-scale fusion, and adopts the Swish activation function to improve training stability. Experimental results demonstrate that PDDA achieves 86.9% mAP@0.5 with a throughput of 12 fps, outperforming several mainstream detectors while maintaining practical efficiency for direct, continuous monitoring.

KEYWORDS

silicon-based ultraviolet sensor, true discharge, object detection, multi-scale feature fusion, indus-trial safety monitoring

INTRODUCTION

True discharge is an early manifestation of insulation deterioration and is closely related to the risk of subsequent flashover and equipment failure. In industrial production scenarios, such as textile manufacturing, where high-speed machinery and complex electrical systems operate continuously, real-time discharge detection is crucial for ensuring production continuity and safety. In many deployments, silicon-based UV sensors are paired with embedded processors for online monitoring, which places strict constraints on model size and inference latency. With the rapid development of silicon-based ultraviolet sensors, it has become feasible to directly capture the ultraviolet radiation emitted by discharge events and to perform non-contact, continuous

monitoring in the field. Compared with conventional inspection that relies on manual interpretation, silicon-based UV sensing can provide more timely discharge evidence, but the raw UV images often contain weak targets, sparse photon responses, and background noise, which makes reliable localization challenging. Therefore, an efficient and robust detection algorithm is required to automatically identify true discharge regions from silicon-based UV data while meeting the real-time requirements of practical monitoring systems.

There has been substantial research on discharge detection and evaluation. Guo Jianxin et al. combined Local Mean Decomposition and Long Short-Term Memory networks to classify discharge conditions [1]. Tan Xinghua et al. improved convolutional kernels using multiple nonlinear transformations, which reduced model complexity and enhanced detection accuracy [2]. Wang Shenghui and Lu Fangcheng introduced ultraviolet discharge imaging with deep learning for severity assessment by optimizing SSD and YOLOv3 through adaptive learning-rate strategies [3,4]. More recently, Yang Yang et al. improved YOLOv8 using Mosaic-9 augmentation, a Ghost-Net backbone, and alternative activation and loss designs such as GeLU and SIoU, achieving faster inference for discharge evaluation [5]. However, for silicon-based UV monitoring, true discharge targets are typically small and may coexist with artifacts caused by noise and scene textures, so further algorithmic refinement is still necessary to improve accuracy without sacrificing deployability.

Despite this progress, most existing studies are designed for laboratory analysis or offline evaluation, and their pipelines often assume relatively clean measurements or rely on manual screening. When silicon-based UV sensors are used for direct monitoring, the imaging process is dominated by sparse photon counts, sensor noise, and background clutter. Consequently, true-discharge signatures often appear as tiny and weak targets that are easily missed or confused with spurious responses.

In addition, in industrial online monitoring, the constraints are primarily deployment budgets—real-time latency, memory footprint, and power/thermal limits for continuous 24/7 operation—rather than peak compute capability alone. Therefore, we target embedded edge deployments where models must meet these budgets on-device while maintaining reliable detection. Methods that improve accuracy by substantially increasing model depth or introducing heavy attention operations may be difficult to deploy in this setting. Therefore, it remains necessary to develop a lightweight yet robust detector that can operate directly on silicon-based UV imagery and reliably identify true-discharge regions in real time.

To address these requirements, this paper builds on YOLOv8 and designs targeted improvements for silicon-based UV discharge monitoring [6]. The proposed approach enhances feature discrimination under low

signal-to-noise conditions and strengthens cross-scale context integration for small and densely distributed targets.

The main contributions of this paper are summarized as follows:

1. A discharge detection framework is developed for direct monitoring with silicon-based UV sensors, emphasizing deployability on resource-constrained platforms.
2. EMA attention is embedded into the bottleneck to model pixel-level dependencies and suppress background interference, improving sensitivity to weak discharge cues [7].
3. A Cross-level Context Fusion Module is introduced to replace the original neck, enabling more effective cross-scale fusion for clustered small targets with low computational overhead [8].
4. The Swish activation function is adopted in convolutional layers to improve optimization stability and mitigate dead-neuron effects, further boosting detection performance [9].

The remainder of this paper is organized as follows. Section 2 presents the proposed precision discharge detection algorithm and its key components. Section 3 reports experimental settings and comparative results. Section 4 concludes the paper and discusses future work.

PRECISION DISCHARGE DETECTION ALGORITHM

YOLOv8 Target Detection Algorithm

YOLOv8 is a representative one-stage detector that unifies classification and localization in a single forward pass, making it suitable for real-time true-discharge monitoring. It follows a backbone-neck-head design. The backbone extracts hierarchical feature maps at multiple resolutions, the neck aggregates cross-scale information to build a feature pyramid, and the head predicts category scores and bounding boxes for different target sizes. For silicon-based UV sensing, this multi-scale representation is important because true-discharge signatures are often tiny and their appearance can vary with distance, exposure, and operating conditions.

In YOLOv8, the backbone is built from efficient convolutional blocks such as C2f modules and a spatial pyramid pooling layer, which extract both local details and higher-level context. The neck typically combines a feature pyramid with path aggregation to propagate semantics downward and details upward, forming multi-scale features for detection. Predictions are produced on multiple feature levels so that small discharge spots and larger luminous regions can be handled simultaneously, and non-maximum suppression is applied during post-processing to remove redundant boxes.

Compared with earlier YOLO variants, YOLOv8 employs an anchor-free and decoupled detection head. It directly regresses box locations without predefined anchors, which reduces hyperparameter dependence and improves generalization. The classification and regression branches are separated to mitigate task interference and to stabilize training. In addition, localization is optimized with an IoU-based regression objective together with Distribution Focal Loss, enabling a finer grained representation of box boundaries and improving localization quality for small targets.

However, when applied to silicon-based UV images, the baseline YOLOv8 can still struggle with weak signals, dense clustered discharges, and background noise, which may cause missed detections and false alarms. These challenges motivate the improvements proposed in this paper, including feature enhancement, stronger cross-level fusion in the neck, and a more stable activation design, to achieve accurate and deployable true-discharge detection. The overall structure is shown in Figure 1.

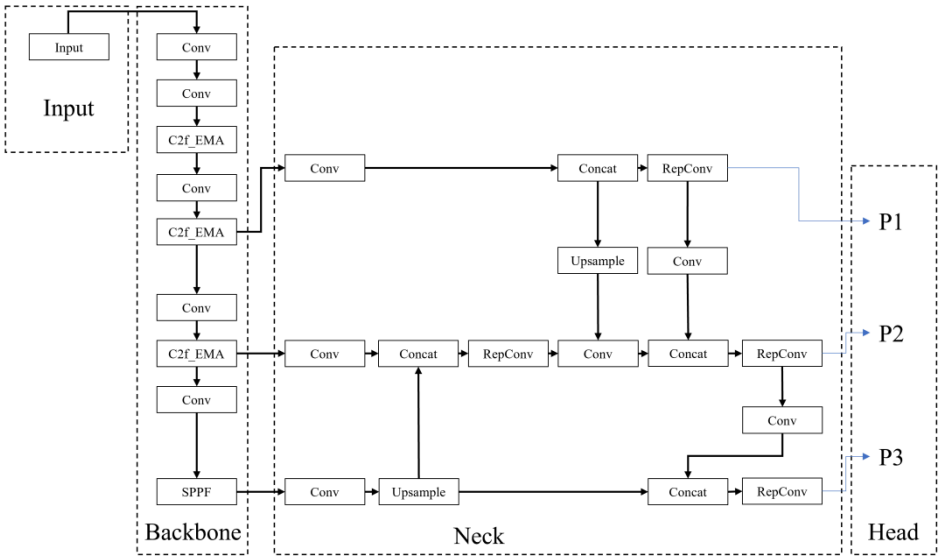

Figure 1. PDDA Network Structure

EMA Attention Mechanism

Raw inputs used in deep learning models often contain substantial irrelevant information. Attention mechanisms mitigate this by dynamically reweighting features so that the network emphasizes task-relevant local regions and suppresses redundant interference. The EMA attention mechanism is an efficient feature-enhancement module that improves a model's perception of complex scenes through multi-scale feature

aggregation and cross-dimension interaction. It also employs parallel sub-structures to reduce reliance on sequential processing.

EMA retains the shared 1×1 convolution component from the Coordinate Attention (CA) module [10]. In addition, to aggregate multi-scale spatial structural cues, it introduces a parallel branch that places a 3×3 kernel alongside the 1×1 branch to enable fast responses. This branch is referred to as the 3×3 branch. By preserving channel information while lowering computational cost, EMA is particularly effective at capturing global context and long-range dependencies. The architecture of EMA is illustrated in Figure 2.

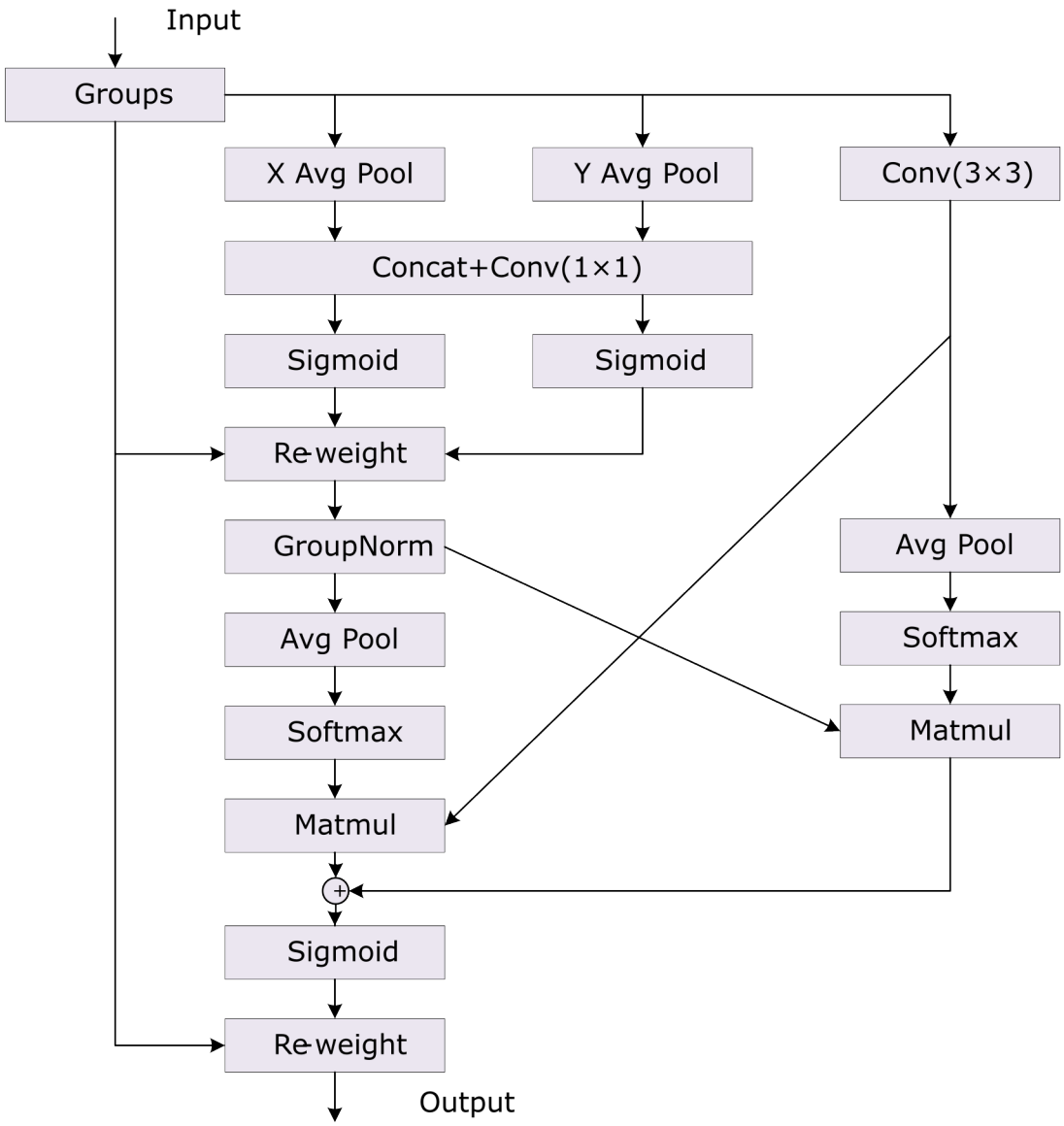

Figure 2. EMA Mechanism

In this work, EMA is integrated into the original Bottleneck module by inserting the attention mechanism after the two convolution layers to strengthen feature extraction. Accordingly, the modified C2f module is redesigned as the proposed C2f-EMA module.

EMA enables the network to model pixel-level dependencies by assigning higher weights to regions associated with discharge and lower weights to background disturbances. This selective emphasis suppresses background noise and enhances the overall performance of the detection model.

CCFM Neck Network

True discharge targets often appear densely distributed and share highly similar visual patterns, which easily leads to feature confusion in imaging-based detection. In practical measurements, true discharge responses can be close to background artifacts and structural textures, making it difficult to separate adjacent sources with similar appearances. Although YOLOv8 employs an improved PANet structure with Adaptive Spatial Feature Fusion for multi-scale weighting, its fusion routes are relatively fixed and its ability to model nonlinear interactions and contextual dependencies across feature levels remains limited. As a result, the model may produce ambiguous localization or misclassification when distinguishing closely spaced true discharge points with similar textures. To accurately separate densely clustered true discharge sources, stronger cross-level feature integration is required. Therefore, this study introduces a Cross-level Context Fusion Module as the neck network to enhance cross-scale contextual interaction and feature fusion, thereby improving true discharge detection performance.

CCFM is a feature fusion neck network structure proposed by Zhao Yian et al. It is more efficient and enables more thorough feature fusion compared to traditional feature fusion pyramid structures like PANet and BiFPN. Its main structure can be represented in a simplified manner by Figure 3 below:

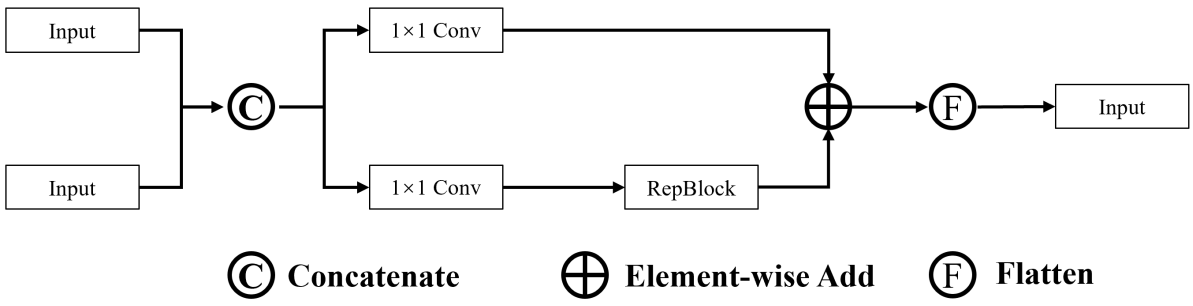

Figure 3. CCFM Network Structure

The figure illustrates that CCFM is designed to combine backbone-produced feature tensors that vary in spatial scale and semantic depth into one strong feature stream that the detection head can directly use. To meet this aim, CCFM avoids cross-scale attention commonly used in Transformer-style designs and instead adopts lightweight convolutional routes for feature blending. CCFM reduces the reliance on computationally expensive attention by replacing heavy/global attention operations in the fusion stage with lightweight convolutional feature modulation. Although the backbone includes EMA attention, it is a lightweight local attention mechanism; overall, the proposed design keeps the total computational budget bounded while improving accuracy. Its main building unit is the fusion block. Each block receives two neighboring pyramid levels, applies a 1×1 convolution to match channel counts, and then uses several efficient RepConv layers to reshape and mix the information. After that, the two branches are combined by pointwise summation to produce a single output.

By stacking multiple fusion blocks in an FPN or PAN style, CCFM gradually aggregates cues from all feature levels through a descending or ascending fusion pass, while high-level semantics and fine details are repeatedly injected and sharpened. Since the whole module is convolution based, it bypasses the attention cost that grows quadratically with sequence length. RepConv adopts a multi-branch form during training to strengthen representation, but it can be re-parameterized into a single standard convolution at inference, which improves runtime efficiency while preserving accuracy. Consequently, Figure 1 shows that this work replaces the YOLOv8 neck fusion stage with CCFM to support fast and reliable multi-scale target detection.

Swish Activation Function

In the YOLO series and even the most advanced deep learning object detection algorithms currently, the commonly used activation function is the ReLU function, which is defined in Eq (1).

$$F_{ReLU} = \max(0, X) \tag{1}$$

As can be inferred from the expression, ReLU yields a zero derivative when the input falls below zero. Once the pre-activation values enter this negative range during training, the gradient for that unit becomes zero and no error signal is propagated forward through it. Consequently, the affected units stop reacting to the data and their weights no longer get updated, which can lead to the well-known dead-neuron problem. This phenomenon can noticeably weaken optimization efficiency and degrade training outcomes.

To mitigate this limitation, this work adopts the Swish activation function as a substitute for ReLU. The definition of Swish is given in Eq (2).

$$F_{\text{Swish}} = x\,\sigma(\beta x) = x\frac{1}{1+e^{-\beta x}} \tag{2}$$

Where β is a trainable parameter that updates during model training.

As shown, Swish is unbounded in the positive direction while remaining bounded on the negative side, similar to ReLU. It helps alleviate gradient saturation and can offer a stronger regularizing effect. Unlike ReLU, Swish is smooth and differentiable, which reduces the risk of dead neurons caused by zero gradients in the negative region. Therefore, this paper replaces ReLU with Swish in the convolutional layers.

EXPERIMENTS AND ANALYSIS OF RESULTS

The experiment was conducted using a real discharge dataset collected by the silicon-based ultraviolet sensor, which contains 3,950 images. These images were divided into the training, validation, and test sets in a ratio of 8:1:1. All images were labeled with bounding boxes indicating the discharge area. The model was trained and evaluated under consistent settings to ensure a fair comparison. The detection accuracy was reported using mAP at an IoU threshold of 0.5, and the running efficiency was measured in terms of frames per second in the same inference environment. The ablation experiments and comparative tests conducted in this paper were all carried out using this dataset to ensure fairness.

Experimental Environment, Hyperparameter Setting

Model training was carried out on a high-end workstation featuring an NVIDIA A100 GPU (40 GB memory), dual AMD EPYC 7713 CPUs, and 256GB system RAM. The training stack ran on CentOS 8.4 with PyTorch 1.12.1, CUDA 11.6, and Python 3.9.7.

To better approximate real-world deployment, inference and performance benchmarking were executed on an NVIDIA Jetson AGX Orin device. The platform used JetPack 5.0.2 on Ubuntu 20.04, together with a PyTorch-compatible runtime for on-device inference. At the same time, to ensure compatibility with the on-site usage environment, we have limited the power of the edge computing module to 20W.

For optimization, a fixed set of hyperparameters was used to promote stable convergence. The model was trained for 200 epochs with a batch size of 32, using the Adam optimizer. The learning rate was initialized at 1×10^{-4} , and the momentum term was set to 0.937.

Ablation Experiment

To verify the effectiveness of the proposed improvements, an ablation study is performed based on the YOLOv8 baseline. As summarized in Table 1, Net-1 introduces the EMA attention mechanism to enhance feature representation and suppress background interference. Net-2 further replaces the original neck with CCFM to strengthen cross-scale fusion for small and clustered discharge targets. Finally, PDDA integrates EMA, CCFM, and the Swish activation function to form the complete model.

Table 1. PDDA Ablation Experiment

Model	EMA	CCFM	Swish	mAP@0.5	fps
YOLOv8				81.2	21
Net-1	√			83.3	16
Net-2	√	√		85.7	13
PDDA	√	√	√	86.9	12

Table 1 shows that EMA improves the baseline from 81.2% to 83.3% mAP, indicating that pixel-level reweighting helps the detector focus on true-discharge regions and reduces interference from background responses. With CCFM added, Net-2 reaches 85.7% mAP, which suggests that stronger cross-level fusion benefits small targets by injecting semantic cues into high-resolution feature maps. After replacing ReLU with Swish, the complete PDDA model achieves the best accuracy of 86.9% mAP, while maintaining 12 fps. Although PDDA reduces throughput from 21 fps to 12 fps (−42.9%), it increases mAP@0.5 from 81.2% to 86.9% (+ 5.7 percentage points). Under an online monitoring requirement of ≥ 10 fps on Jetson AGX Orin, PDDA satisfies real-time constraints while providing a measurable accuracy gain; therefore, the accuracy–speed trade-off is acceptable for industrial deployment.

In terms of efficiency, adding EMA, CCFM, and Swish gradually reduces the throughput from 21 fps to 12 fps. The decrease mainly comes from the extra convolutional branches and deeper cross-scale fusion paths. Nevertheless, the final model maintains double-digit speed, which is adequate for most monitoring pipelines where discharge evolution is not instantaneous.

Algorithm Comparison Experiment

To further evaluate the proposed method, PDDA is compared with representative two-stage detectors, transformer-based detectors, and mainstream YOLO variants. The algorithms used in this experiment were all executed on the Jetson Orin AGX edge computing module. Here, Net and Net-2 denote improved YOLOv8-

based approaches reported in prior studies and are used as external baselines, which should be distinguished from the intermediate ablation variants in Table 2 [2,5]. The results are reported in Table 2 in terms of both mAP@0.5 and inference speed.

Table 2. Comparison Experiment

Model	mAP@0.5	fps
Faster-RCNN [11]	79.1	2
DETR [12]	80.9	4
YOLOv5	66.2	33
YOLOv6 [13]	78.1	7
YOLOv7 [14]	82.3	8
YOLOv8 [6]	81.2	21
Net [2]	75.1	20
Net-2 [5]	65.4	12
PDDA	86.9	12

As shown in Table 2, Faster R-CNN and DETR achieve competitive accuracy but run far below real-time speed, which limits their suitability for online monitoring. Among the YOLO baselines, YOLOv5 delivers the highest frame rate but suffers a substantial accuracy drop on silicon-based UV images, reflecting the difficulty of detecting weak discharge patterns. YOLOv7 improves accuracy but its speed is significantly lower than YOLOv8. The proposed PDDA achieves the best detection accuracy of 86.9% mAP, outperforming the YOLOv8 baseline by 5.7 percentage points, while maintaining a practical throughput of 12 fps. These results demonstrate that the introduced feature enhancement and cross-scale fusion are effective for true-discharge monitoring based on silicon-based UV sensing.

In addition, PDDA shows clear advantages over the lightweight baselines Net and Net-2, indicating that simply compressing the network is insufficient for silicon-based UV data without targeted feature enhancement. Overall, PDDA improves accuracy while keeping computation at a manageable level, making it more suitable for deployment alongside silicon-based UV sensing hardware than heavier two-stage or transformer-based detectors.

CONCLUSIONS

This paper proposes PDDA, an accurate true-discharge detection method tailored for silicon-based UV sensors. By taking YOLOv8 as the baseline and introducing EMA attention, a CCFM neck, and the Swish activation

function, the proposed model enhances sensitivity to weak and small discharge targets and suppresses background interference. Experiments show that PDDA deployed on Jetson AGX Orin achieves 86.9% mAP@0.5 at 12 fps, meeting the real-time monitoring constraint while improving accuracy by 5.7 percentage points over YOLOv8; this quantifies the deployment-acceptable accuracy–speed trade-off for continuous industrial monitoring. The results of this study provide a robust algorithmic foundation for the intelligent safety inspection of industrial equipment, including potential applications in textile machinery monitoring. Future work will focus on expanding the dataset across more operating conditions, including specific scenarios like aging equipment in weaving workshops. improving robustness to extreme noise and overexposure, and exploring multi-sensor fusion to further enhance early-warning capability.

Author Contributions

Conceptualization, LYY and DCL; Data curation, LYY; Funding acquisition, LY, LYY, DCL; Methodology, LY and LYY; Project administration, LY; Software, LY; Su-pervision, LYY; Validation, DCL; Visualization, LYY; Writing – original draft, LY; Writing – review & editing, LYY.

Conflicts of Interest

The authors declare no conflict of interest.

Funding

This study was supported by the State Grid Electric Power Co., Ltd. Science and Technology Project (Project No.: 5700-202413274A-1-1-ZN).

Availability of data and material

The datasets used and/or analyzed during the current study are available from the corresponding author on reasonable request.

Acknowledgements

None.

REFERENCES

[1] Guo J, Zhao Y, Wang Z, Ding L. Recognition method of local discharge patterns of typical defects in pin-type insulators based on LMD and LSTM. Southern Power System Technology. 2021;15(8):95-105. doi: 10.13648/j.cnki.issn1674-0629.2021.08.012

[2] Tan X, Chen R, Ding W, Zhang G. Non-destructive detection of electrical insulator discharges based on improved convolutional neural networks. Automation & Instrumentation. 2023;38(4):88-91, 97. doi: 10.19557/j.cnki.1001-9944.2023.04.018

[3] Wang S, Dong X, Wang X, Jin C, Sun K, Lü F. Evaluation of discharge severity in suspension insulators based on improved SSD algorithm and ultraviolet imaging. Journal of North China Electric Power University (Natural Science Edition). 2023;50(5):35-44. doi: 10.3969/j.issn.1007-2691.2023.05.05

[4] Lü F, Niu L, Wang S, Chu Y. Evaluation of discharge severity in porcelain suspension insulators based on ultraviolet imaging and improved YOLOv3. High Voltage Engineering. 2021;47(2):377-386. doi: 10.13336/j.1003-6520.hve.20200674

[5] Yang Y, Geng S, Cheng C, Yang X, Wu P, Han X, Zhang H. An edge algorithm for assessing the severity of insulator discharges using a lightweight improved YOLOv8. Journal of Electrical Engineering & Technology. 2025;20(1):807-816. doi: 10.1007/s42835-024-02021-4

[6] Varghese R, Sambath M. YOLOv8: A novel object detection algorithm with enhanced performance and robustness. In: Proceedings of the 2024 International Conference on Advances in Data Engineering and Intelligent Computing Systems (ADICS 2024); 2024 Mar 28-29; Chennai, India. Piscataway (NJ): IEEE; 2024. p.1-6. doi: 10.1109/ADICS58448.2024.10533619

[7] Ouyang D, He S, Zhang G, Luo M, Guo H, Zhan J, Huang Z. Efficient multi-scale attention module with cross-spatial learning. In: Proceedings of the IEEE International Conference on Acoustics, Speech and Signal Processing (ICASSP 2023); 2023 Jun 4-9; Rhodes Island, Greece. Piscataway (NJ): IEEE; 2023. p.1-5. doi: 10.1109/ICASSP49357.2023.10096516

[8] Zhao Y, Lv W, Xu S, Wei J, Wang G, Dang Q, Liu Y, Chen J. DETRs beat YOLOs on real-time object detection. In: Proceedings of the IEEE/CVF Conference on Computer Vision and Pattern Recognition (CVPR 2024); 2024 Jun 16-22; Seattle, WA, USA. Piscataway (NJ): IEEE; 2024. p.16965-16974. doi: 10.1109/CVPR52733.2024.01602

[9] Ramachandran P, Zoph B, Le QV. Searching for activation functions. arXiv preprint. 2017. https://arxiv.org/abs/1710.05941

[10] Wang CY, Liao HYM, Wu YH, Chen PY, Hsieh JW, Yeh IH. CSPNet: A new backbone that can enhance learning capability of CNN. In: Proceedings of the IEEE/CVF Conference on Computer Vision and Pattern Recognition Workshops; 2020. p. 390–391.Available from: https://doi.org/10.1109/CVPRW50498.2020.00203

[11] Ren S, He K, Girshick R, Sun J. Faster R-CNN: Towards real-time object detection with region proposal networks. IEEE Transactions on Pattern Analysis and Machine Intelligence. 2017;39(6):1137-1149. doi: 10.1109/TPAMI.2016.2577031

[12] Carion N, Massa F, Synnaeve G, Usunier N, Kirillov A, Zagoruyko S. End-to-end object detection with transformers. In: Vedaldi A, Bischof H, Brox T, Frahm J-M, editors. Computer Vision – ECCV 2020. Proceedings of the ECCV 2020; 2020 Aug 23–28; Glasgow, UK. Cham: Springer; 2020. p. 213–229. Available from: https://doi.org/10.1007/978-3-030-58452-8_13

[13] Li C, Li L, Jiang H, Weng K, Geng Y, Li L, et al. YOLOv6: A single-stage object detection framework for industrial applications. arXiv preprint. 2022. https://arxiv.org/abs/2209.02976

[14] Wang C-Y, Bochkovskiy A, Liao H-YM. YOLOv7: Trainable bag-of-freebies sets new state-of-the-art for real-time object detectors. In: Proceedings of the IEEE/CVF Conference on Computer Vision and Pattern Recognition (CVPR 2023); 2023 Jun 17–24; Vancouver, Canada. Piscataway (NJ): IEEE; 2023. p. 7464–7475. Available from: https://openaccess.thecvf.com/content/CVPR2023/papers/Wang_YOLOv7_Trainable_Bag-of-Freebies_Sets_New_State-of-the-Art_for_Real-Time_Object_Detectors_CVPR_2023_paper.pd